

Potential Process Control Issues With Abatacept

James T. Isaacs¹, Philip J. Almeter^{1,2}, Aaron N. Hunter¹, Thomas A. Lyman¹, Stephanie P. Zapata¹, Bradley S. Henderson¹, Seth A. Larkin^{1,2}, Lindsey M. Long^{1,2}, Megan N. Bossle^{1,2}, Smaran A. Bhaktawara^{1,2}, Matthew F. Warren^{1,2}, Austin M. Lozier^{1,2}, Joshua D. Melson^{1,2}, Savannah R. Fraley^{1,2}, Eunice Hazzel L. Relucio^{1,2}, Margaret A. Felix¹, Jeffrey W. Reynolds³, Ryan W. Naseman^{1,2}, Thomas L. Platt^{1,2}, Robert A. Lodder^{4,*}

University of Kentucky
Lexington, KY

1. Department of Pharmacy Services, University of Kentucky HealthCare, Lexington, KY 40536
2. Pharmacy Practice & Sciences, College of Pharmacy, University of Kentucky, Lexington, KY 40536
3. Department of Finance, University of Kentucky HealthCare, Lexington, KY
4. Department of Pharmaceutical Sciences, University of Kentucky, Lexington, KY 40536

*Author to whom correspondence should be addressed. Email: Lodder @ g.uky.edu
ORCID 0000-0001-6133-7561

RAPID COMMUNICATION

Abstract

Abatacept is a medication administered through intravenous infusion. It is supplied as a sterile, white, preservative-free, freeze-dried powder. Each vial of drug contains 250 mg abatacept, maltose, monobasic sodium phosphate, and sodium chloride for administration. Abatacept is a fusion protein consisting of the extracellular domain of CTLA-4 linked to the modified Fc portion of human immunoglobulin G1. It is produced using recombinant DNA technology. Abatacept is indicated for moderately to severely active rheumatoid arthritis in adults and polyarticular juvenile idiopathic arthritis in pediatric patients 6 years of age and older. It can be used as monotherapy or in combination with other disease-modifying antirheumatic drugs or methotrexate.

Inter-lot variability was detected in a library of 132 vials spread across 34 lots of abatacept-maltose for injection by the University of Kentucky Drug Quality Task Force. A subcluster detection test was run on 13 vials that were shown to be an outlier group ($r_{in}=0.9940$, $r_{test}=0.9551$, $r_{lim}=0.9865$, $p=0.02$). Five of these vials individually appeared 4 or more standard deviations from the library cluster.

Introduction

The University of Kentucky's (UK) Drug Quality Task Force (DQTF) was established in August of 2019 to engage in consumer-level quality assurance screening for drugs used within UK HealthCare's pharmacies ([Isaacs, 2023a](#)). DQTF currently screens medications using Fourier transform near-infrared spectrometry (FTNIR) and Raman spectrometry for potential quality defects indicated by variability in absorbance peak intensities and locations. Through years of continuous monitoring, DQTF has assembled a spectral library containing medications typically used in a health system setting. Statistical analyses using the DQTF spectral library are performed to identify potential intra-lot and inter-lot variability in medications under review. Using Medwatch and publications in the scientific literature, DQTF reports its findings in an effort to hold manufacturers accountable for GMP requirements and to improve patient outcomes by providing information on quality to augment the information on price that is already available. The increasing transparency is designed to improve the pharmaceutical supply chain.

Drug Product

ORENCIA® (abatacept) lyophilized powder for intravenous infusion is supplied as a sterile, white, preservative-free, lyophilized powder for intravenous administration (see [Figure 1](#)). Following reconstitution of the lyophilized powder with 10 mL of Sterile Water for Injection, USP, the solution of abatacept is clear, colorless to pale yellow, with a pH range of 7.2 to 7.8. Each single-use vial of ORENCIA provides 250 mg abatacept, maltose (500 mg), monobasic sodium phosphate (17.2 mg), and sodium chloride (14.6 mg) for administration ([FDA, 2013](#)).

Abatacept is a soluble fusion protein that consists of the extracellular domain of human cytotoxic T-lymphocyte-associated antigen 4 (CTLA-4) linked to the modified Fc (hinge, CH2, and CH3 domains) portion of human immunoglobulin G1 (IgG1). Abatacept is produced by recombinant DNA technology in a mammalian cell expression system. The apparent molecular weight of abatacept is 92 kilodaltons ([FDA, 2013](#)).

Abatacept is a selective T cell costimulation modulator indicated for moderately to severely active Rheumatoid Arthritis in adults. Abatacept may be used as monotherapy or concomitantly with DMARDs (Disease-Modifying Antirheumatic Drugs) other than TNF (tumor necrosis factor) antagonists, or in moderately to severely active polyarticular juvenile idiopathic arthritis in pediatric patients 6 years of age and older. Abatacept may be used as monotherapy or concomitantly with methotrexate ([FDA, 2013](#)). Abatacept is

also indicated for the treatment of adult patients with active psoriatic arthritis and the prophylaxis of acute graft versus host disease (aGVHD), in combination with a calcineurin inhibitor and methotrexate, in adults and pediatric patients 2 years of age and older undergoing hematopoietic stem cell transplantation (HSCT) from a matched or 1 allele-mismatched unrelated donor. ([BMS, 2021](#))

The lot numbers making up the spectral library were ABL0468, ABL0474, ABL0475, ABM2443, ABN1100, ABQ4878, ABQ4879, ABQ4882, ABS4975, ABS4976, ABS4983, ABU5827, ABV2746, ABV5535, ABW3078, ABW3080, ABW3081, ABW3082, ABX4545, ABX4547, ABX4549, ABX4550, ABY1233, ABY1234, ABY1236, ABZ4262, ACA5143, ACB6446, ACB6447, ACB6448, ACB6449, ACB6450, ACC6785, ACC6787.



Figure 1. Vials of abatacept from lot ACC6785. The drug is a sterile, white, preservative-free, lyophilized powder for intravenous administration.

Background

Recent studies

An open-label, multicenter, 1-year, prospective study (ROSE [Rheumatoid Arthritis with Orencia Trial Toward Sjögren's Syndrome Endocrinopathy]) recently completed ([Tsuboi, 2023](#)). The goal of the study was to clarify the efficacy and safety of intravenous abatacept for glandular and extraglandular involvements in Sjögren's syndrome related to rheumatoid arthritis. The study found that abatacept reduced both glandular and extraglandular involvements, as well as the systemic disease activities and patient-reported outcomes founded on composite measures, in Sjögren's syndrome associated with rheumatoid arthritis.

A preclinical study was conducted on Sprague-Dawley rats to investigate whether improvement of placental function is associated with the reduction of hypertension during a hypertensive pregnancy ([Moustafa, 2023](#)). Timed-pregnant Sprague Dawley rats were divided into two groups: normotensive rats and rats implanted with a mini-osmotic pump infusing sFlt-1 and sEng. Different pharmacological treatments were administered during pregnancy, including ABT-627 (ETA receptor blocker), Tempol (superoxide dismutase mimetic), Orencia (T-cell depletion), and IL-17 soluble RC (IL-17 blocker). Blood pressure was measured, and placental samples were analyzed for various growth factors. The results showed that the pharmacological interventions significantly reduced blood pressure, but their effect on placental dysfunction was mixed. Therefore, further studies are required to understand the impact of other interventions on placental dysfunction and pregnancy outcomes.

A recently published Cochrane systematic review and analysis that focused on the efficacy and safety of abatacept for the treatment of rheumatoid arthritis ([Wu, 2023](#)). The review included 13 randomized control trials and involved a total of 5978 adult patients from various geographic regions and races. The purpose of the meta-analysis was to evaluate the comparative effectiveness of abatacept in comparison to other biologic drugs in adults with rheumatoid arthritis.

According to the findings of the meta-analysis, abatacept demonstrated superior health outcomes when compared to other drugs in the treatment of rheumatoid arthritis. This suggests that abatacept may be a more effective treatment option for adults with this condition. It is important to note that the meta-analysis considered various factors, such as the severity of the disease, duration of treatment, and overall patient response.

The publication of this systematic review and meta-analysis provides valuable insights into the potential benefits of using abatacept as a treatment option for rheumatoid arthritis. However, further research and clinical studies may be needed to validate these findings and to explore the long-term safety and efficacy of abatacept in even larger patient populations.

Shortages

In January 2022, Bristol-Myers Squibb (BMS) notified the Therapeutic Goods Administration (TGA) in Australia about abatacept shortages due to manufacturing constraints, component challenges, and shipment delays. The quality of abatacept was not affected ([TGA, 2022](#)). The shortages impacted both subcutaneous presentations (autoinjector and syringe) with limited supply expected in the first half of 2022. There was enough IV abatacept for current patients only. To mitigate the shortage, patients needing subcutaneous abatacept were given a specialist form for pharmacy access. Pharmacists could provide available subcutaneous abatacept without a new prescription using the Serious Scarcity Substitution Instrument. BMS closely monitored and worked to minimize the impact of the shortages, with updates on the Medicine Shortage Reports Database. The TGA collaborated with ARA, Arthritis Australia, and BMS to manage the limited availability, aiming for a gradual increase in availability throughout 2022.

In the fall of 2021, Canada experienced a shortage of abatacept, similar to the one mentioned earlier. This shortage was attributed to a delay in shipping the drug, which can often be a result of manufacturing issues. The shortage persisted for a duration of one month, during which the allocation of abatacept was determined based on historical demand (the available supply was distributed to healthcare providers and patients according to past usage patterns and needs) ([Drug Shortages Canada, 2021](#)).

FDA Medwatch

An FDA Form 3500 Medwatch describing the findings of this Rapid Communication was filed.

Methods

FTNIR (Fourier Transform Near-Infrared) Spectrometry

Using nondestructive analytical techniques, FTNIR spectra were collected from inventory as part of routine medication quality screening. A representative sample of individual vials were selected for screening and noted to be stored under the conditions required by the manufacturer in their original packaging. FTNIR spectra were collected noninvasively and nondestructively through the bottom of the vials using a Thermo Scientific Antaris II FTNIR Analyzer (Waltham, MA, USA) ([Isaacs, 2023b](#)).

Smoothing

Data smoothing is a technique used to remove noise from data. This can be done by fitting a smooth curve to the data, such as a cubic spline. Cubic splines are piecewise cubic polynomials that are continuous and have continuous first and second derivatives. This makes them very smooth and resistant to noise. Cubic splines can be easily fitted to data using least squares ([Matlab, 2023](#)) ([Pollock, 1998](#)).

Multiplicative Scatter Correction (MSC)

Multiplicative scatter correction (MSC) is a widely used spectrometric normalization technique. Its purpose is to correct spectra in such a way that they are as close as possible to a reference spectrum, generally the mean of the data set, by changing the scale and the offset of the spectra ([Isaksson, 1988](#)).

BEST (Bootstrap Error-Adjusted Single-sample Technique)

The BEST calculates distances in multidimensional, asymmetric, nonparametric central 68% confidence intervals in spectral hyperspace (roughly equivalent to standard deviations)([Dempsey, 1996](#)). The BEST metric can be thought of as a "rubber yardstick" with a nail at the center (the mean). The stretch of the yardstick in one direction is therefore independent of the stretch in the other direction. This independence enables the BEST metric to describe odd shapes in spectral hyperspace (spectral point clusters that are not multivariate normal, such as the calibration spectra of many biological systems). BEST distances can be correlated to sample composition to produce a quantitative calibration, or simply used to identify similar regions in a spectral image. The BEST automatically detects samples and situations unlike any encountered in the original calibration, making it more accurate in chemical investigation than typical regression approaches to near-IR analysis. The BEST produces accurate distances even when the number of calibration samples is less than the number of wavelengths used in calibration, in contrast to other metrics that require matrix factorization. The BEST is much faster to calculate as well ($O(n)$ instead of the $O(n^3)$ required by matrix factorization).

Principal Components (PCs)

Principal component analysis is the process of computing the principal components of a dataset and using them to execute a change of basis (change of coordinate system) on the data, usually employing only the first few principal components and disregarding the rest ([Jolliffe, 2016](#)). PCA is used in exploratory data analysis and in constructing predictive models. PCA is commonly utilized for dimensionality reduction by projecting each data point onto only the first few principal components to obtain lower-dimensional data while preserving as much of the original variation in the data as possible. The first principal component is the direction that maximizes the variance of the projected data. The second principal component is the direction of the largest variance orthogonal to the first principal component. Decomposition of the variance typically continues orthogonally in this manner until some residual variance criterion is met. Plots of PC scores help reveal underlying structure in data.

Subcluster Detection

In typical near-infrared multivariate statistical analyses, samples with similar spectra produce points that cluster in a certain region of spectral hyperspace. These clusters can vary significantly in shape and size due to variation in sample packings, particle-size distributions, component concentrations, and drift with time. These factors, when combined with discriminant

analysis using simple distance metrics, produce a test in which a result that places a particular point inside a particular cluster does not necessarily mean that the point is actually a member of the cluster. Instead, the point may be a member of a new, slightly different cluster that overlaps the first. A new cluster can be created by factors like low-level contamination, moisture uptake, or instrumental drift. An extension added to part of the BEST, called FSOB (Fast Son of BEST) can be used to set nonparametric probability-density contours inside spectral clusters as well as outside ([Isaacs, 2023c](#))([Lodder, 1988](#)), and when multiple points begin to appear in a certain region of cluster-hyperspace the perturbation of these density contours can be detected at an assigned significance level using r values, and visualized using quantile-quantile (QQ) plots. The detection of unusual samples both within and beyond 3 SDs of the center of the training set is possible with this method. Within the ordinary 3 SD limit, however, multiple instances are needed to detect unusual samples with statistical significance.

Artificial Intelligence Tools

Artificial intelligence (AI) tools, principally used for background information, include [Bard](#) (Google LLC) and [GPT-4](#) (OpenAI). AI can be used in a variety of ways, including to brainstorm, organize thoughts, develop arguments, and edit.

Results and Discussion

Interlot analysis

The smoothed spectra of 132 vials obtained from 34 lots of abatacept-maltose are shown in [Figure 2](#). Multiplicative scatter correction was applied to the library spectra. At first glance the spectra appear superficially similar. There are some differences between spectra in the water peak at 5150 cm^{-1} .

Distinguishing spectral features between the vials are marked at 4257, 4532, 4763, and 5150 cm^{-1} .

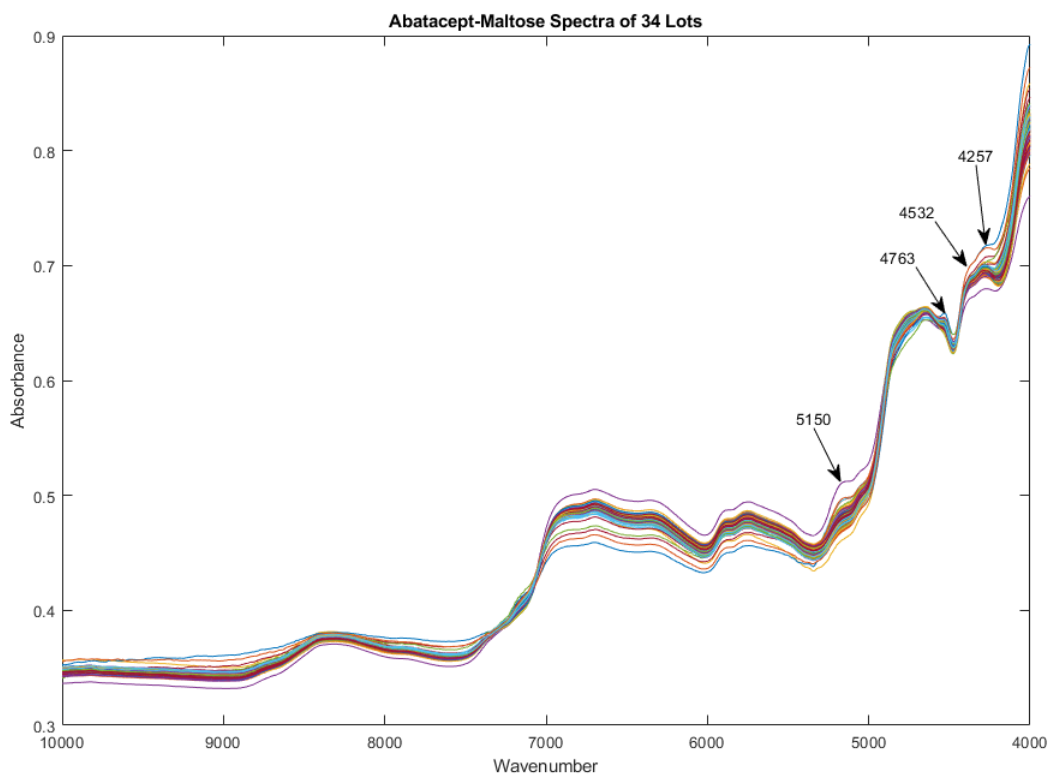


Figure 2. One hundred thirty-two smoothed spectra of 34 lots of abatacept-maltose vials. The areas with differentiating spectral features are marked at 4257, 4532, 4763, and 5150 cm^{-1} .

[Figure 3](#) is a PC scatterplot of the spectra in [Figure 2](#). The putative outliers on PCs 1-3 are vials 10, 14, 55, 56, 57, 68, 89, 90, 114, and 121. In addition, vials 86 and 95 look like outliers on PCs 4-6. Vial 57 is 5.6 SDs from the center of the cluster.

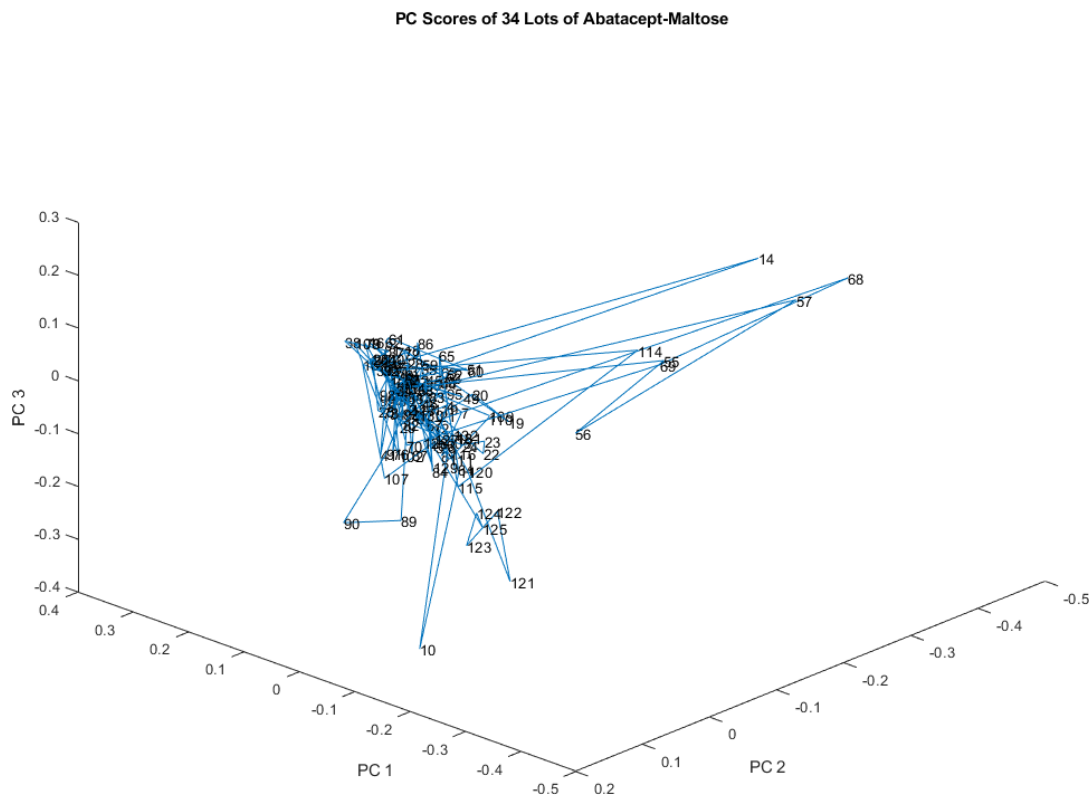


Figure 3. Scatterplot of the scores of the first 3 principal components of the spectral library shown in [Figure 2](#).

[Figure 4](#) compares the mean spectrum (shown in blue) of the 132 vials in 34 lots in the library with the spectrum of vial 57 (shown in red). Vial 57 is 5.6 SDs from the center of the cluster. The difference between vial 57 and the rest of the library is probably not due to moisture content, given the similarity of the peak at 5150 cm^{-1} .

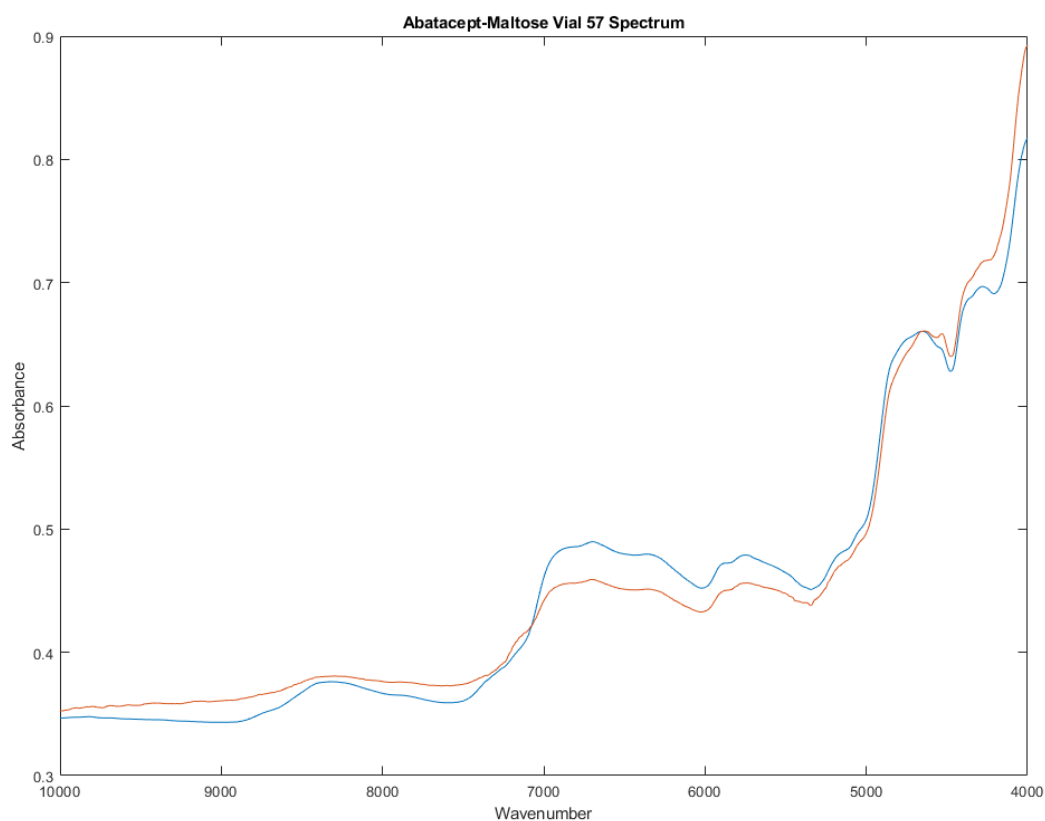


Figure 4. The mean spectrum of the 34 lots in the library is shown in blue, while the spectrum of vial 57 is shown in red. Vial 57 is 5.6 SDs from the center of the cluster. The difference between vial 57 and the rest of the library is probably not due to moisture content, given the similarity of the peak at 5150 cm^{-1} .

On the other hand, vial 18 seems to have more moisture than the average vial in the library. Vial 18 is 4.0 SDs from the center of the cluster of library vials. [Figure 5](#) is a rotated view of the scatterplot of the scores of the first 3 principal components of the spectral library shown in [Figure 3](#). Vial 18 at the bottom of the three dimensional graph is displaced from the center of the library cluster in the direction of moisture. This graph shows that changes in moisture at 5150 cm^{-1} is not well correlated to the peak structures observed at 4763 , 4532 , and 4257 cm^{-1} .

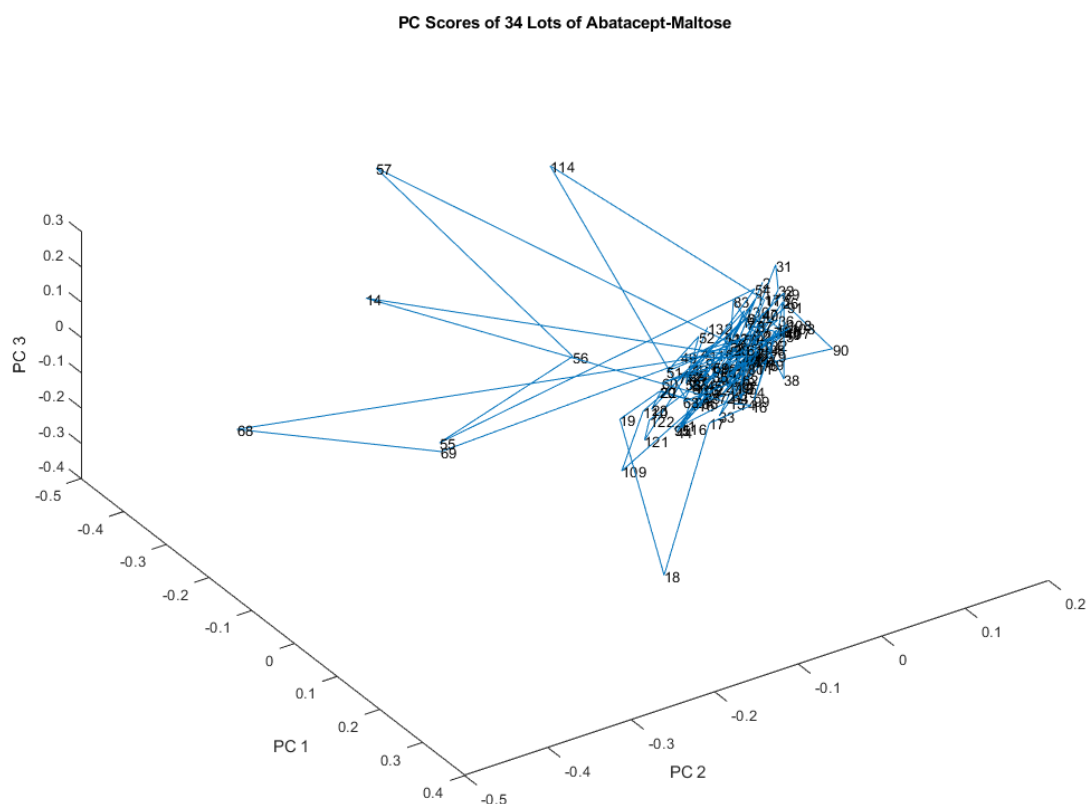


Figure 5. Another rotated view of the scatterplot of the scores of the first 3 principal components of the spectral library shown in [Figure 3](#). Vial 18 is displaced in the direction of moisture.

There is considerable scatter in the directions of vials 14, 55, 56, 57, 68, 69, and 114 from the center of the library, representing different correlations between the absorbance signals at 4257, 4532, and 4763 cm^{-1} . The mean spectrum of the 34 lots in the library is graphed in blue in [Figure 6](#), while the spectrum of vial 18 is graphed in red. Vial 18 is 4.0 SDs from the center of the cluster. The difference between vial 18 and the rest of the 132 vials in the library is probably due to moisture content (note the peak at 5150 cm^{-1}). The peak between 4500 and 5000 cm^{-1} is similar in the spectrum of vial 18 and the mean spectrum of the 34 lots in the library.

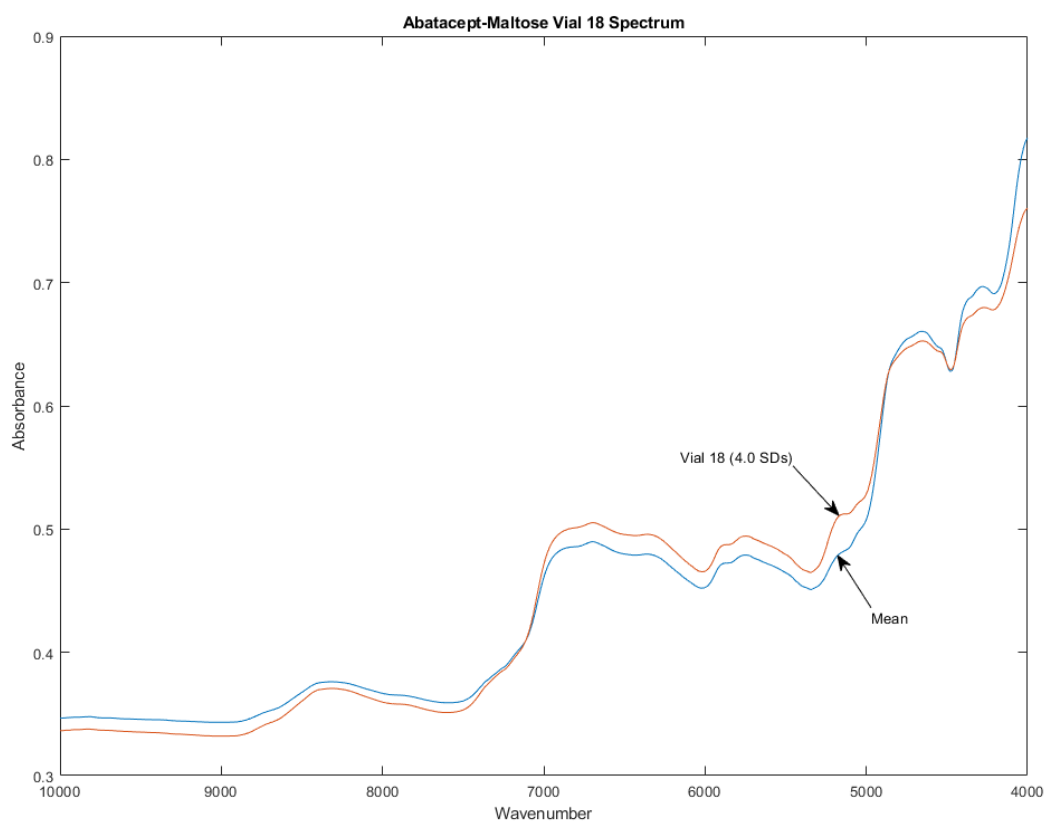


Figure 6. The mean spectrum of the 34 lots in the library is shown in blue, while the spectrum of vial 18 is shown in red. Vial 18 is 4.0 SDs from the center of the cluster. The difference between vial 18 and the rest of the library is probably due to moisture content (note the peak at 5150 cm^{-1}).

[Figure 7](#) graphs the mean spectrum of the 34 lots in the library in blue, while the spectrum of vial 114 is plotted in red. Vial 114 is 3.8 SDs from the center of the cluster. The difference between vial 114 and the rest of the library is probably not due to moisture content, given the similarity of the peak at 5150 cm^{-1} . The peak between 4500 and 5000 cm^{-1} is different in the spectrum of vial 18 and the mean spectrum of the 34 lots in the library.

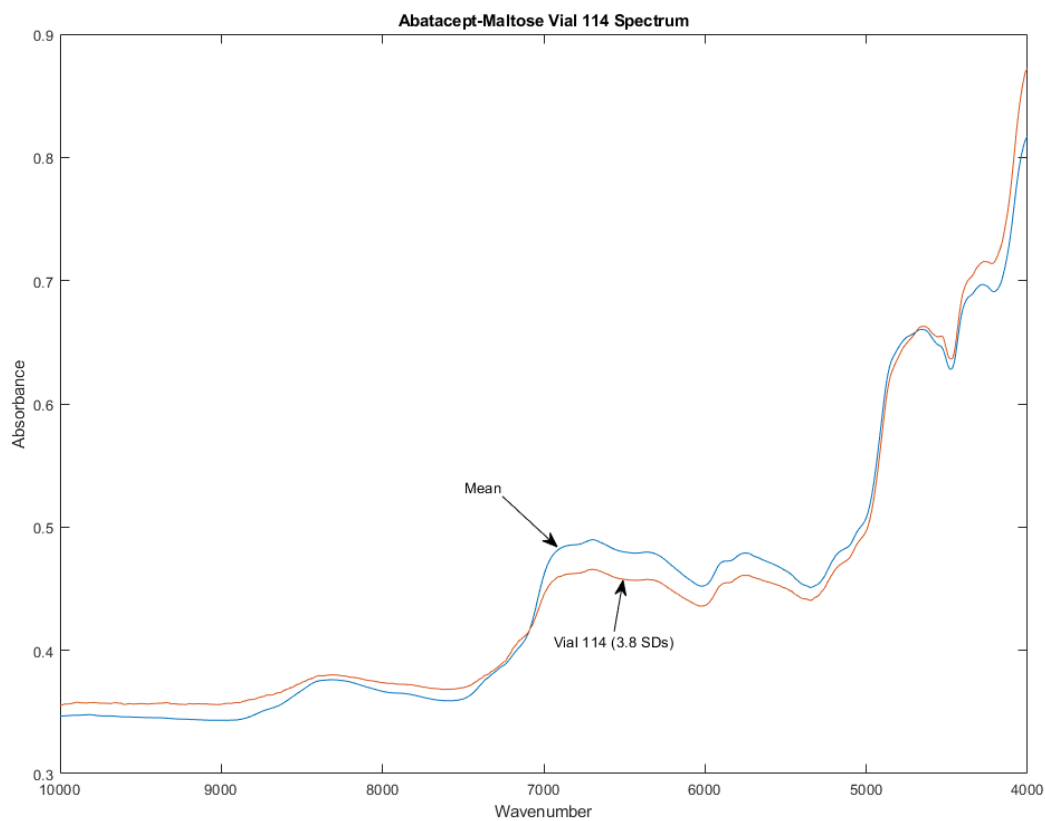


Figure 7. The mean spectrum of the 34 lots in the library is shown in blue, while the spectrum of vial 114 is shown in red. Vial 114 is 3.8 SDs from the center of the cluster. The difference between vial 114 and the rest of the library is probably not due to moisture content, given the similarity of the peak at 5150 cm^{-1} .

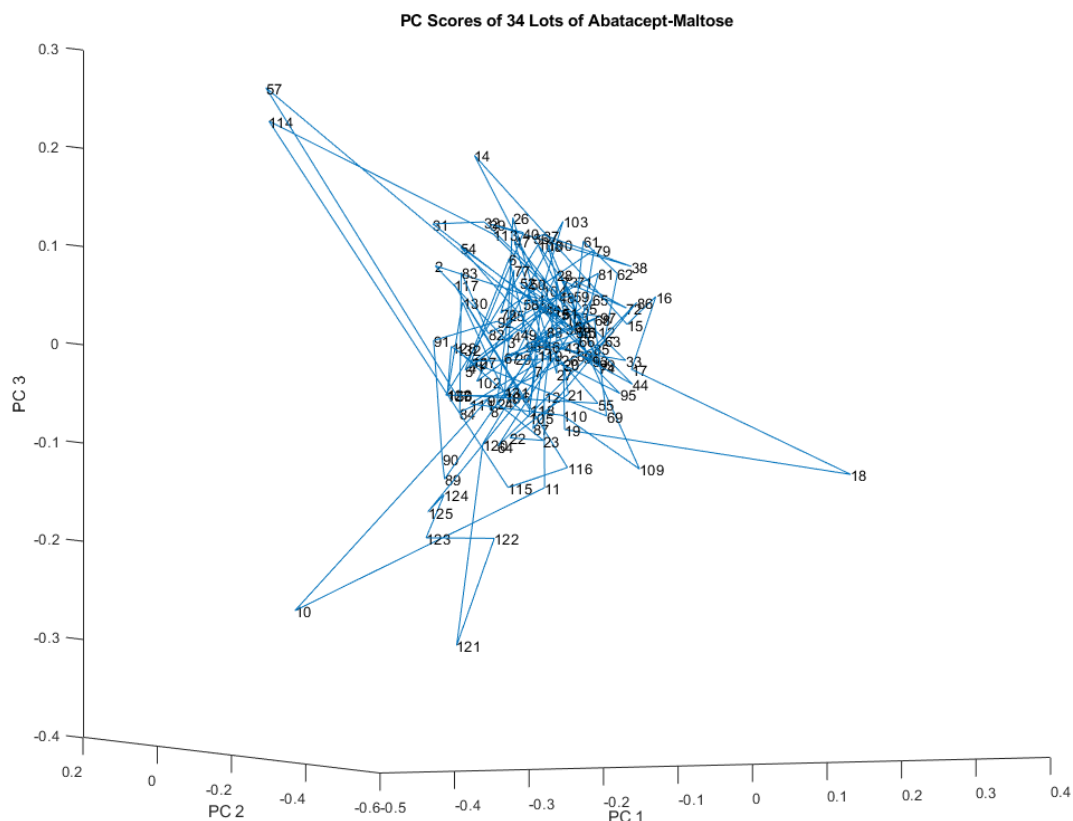


Figure 8. Another view of the scatterplot of the scores of the first 3 principal components of the spectral library shown in Figure 5.

In [Figure 8](#), the outliers are vials 10, 18, 67, 114, and 121. A total of 13 vials in the library appeared to be outliers (almost 10%), so statistical testing was performed on the putative outliers using discriminant analysis with the BEST metric. [Figure 9](#) is the only plot of the scores on the smaller PCs. [Figure 9](#) is a scatterplot of the scores of principal components 4 through 6 of the spectral library shown in [Figure 2](#). Together, PCs 4 through 6 account for less than 1% of the total spectral variation (see [Table 1](#)). The apparent outliers are vials 10, 18, 55, 69, 86, and 95.

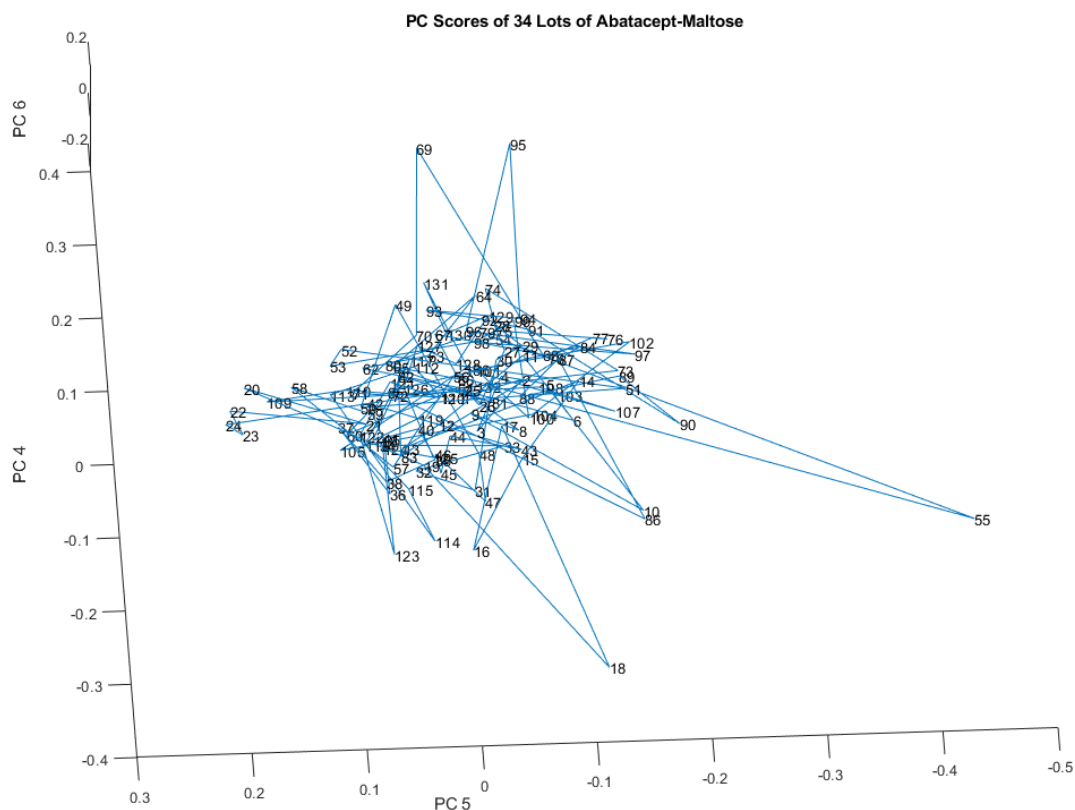


Figure 9. Scatterplot of the scores of principal components 4 through 6 of the spectral library shown in Figure 2. The apparent outliers are vials 10, 18, 55, 69, 95, 10, 86

Table 1: Variation accounted for by each of the principal components of the library spectra

PC Number	Variation in this PC	Cumulative PC Variation
1	0.8090	0.8090
2	0.1071	0.9161
3	0.0547	0.9707
4	0.0157	0.9865
5	0.0049	0.9914
6	0.0025	0.9938

The subcluster detection test was run on the 13 apparent outliers in the space defined by PCs 1 through 3. The mean correlation coefficient for the spectral library (training set) replicates was 0.9940, with a standard deviation of 0.0037. The 98% confidence limit on the training samples was 0.9865. The correlation coefficient for the QQ plot (see [Figure 10](#)) of the spectral library

replicates vs. the apparent outlier replicates was 0.9551, so the spectral library replicates and the apparent outlier replicates are drawn from different distributions. Other words, as a group, the apparent outliers constitute a distinct subcluster of the spectral library, with a different location and scale. This outlier group is larger in terms of volume occupied in PC hyperspace than the spectral library ([Isaacs, 2023c](#)).

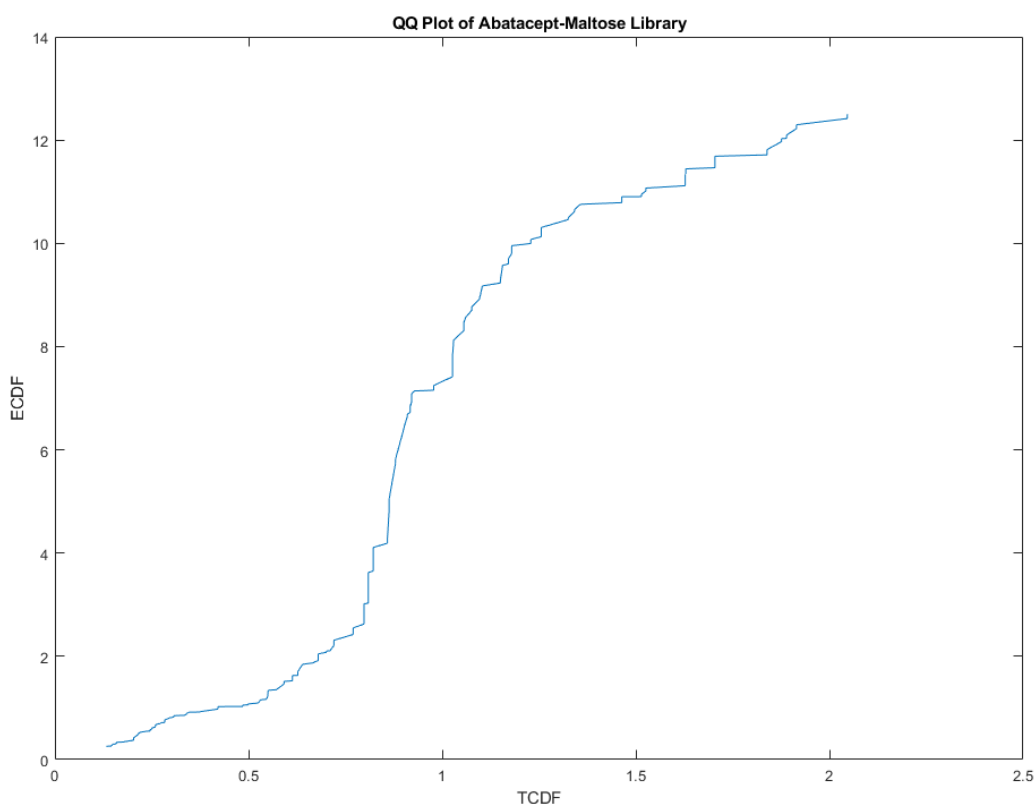


Figure 10. QQ plot from the subcluster detection test for the spectral library vs. the apparent outliers. PCs 1-3, mean=0.9940, SD=0.0037, 98% limit is 0.9865. $r=0.9551$ so the 2 groups do not match. If the two groups matched, the QQ plot would show a straight line with a slope of one and an intercept of zero.

After measuring distances in SDs to each vial, however, only 5 of the apparent outliers are outliers as individual vials. These five vials (and their distances in SDs from the center) are: vial 10 (4.0 SDs), vial 14 (3.6 SDs), vial 18 (5.1 SDs), vial 57 (7.3 SDs), and vial 114 (5.3 SDs).

PC Loadings for the Spectral Library

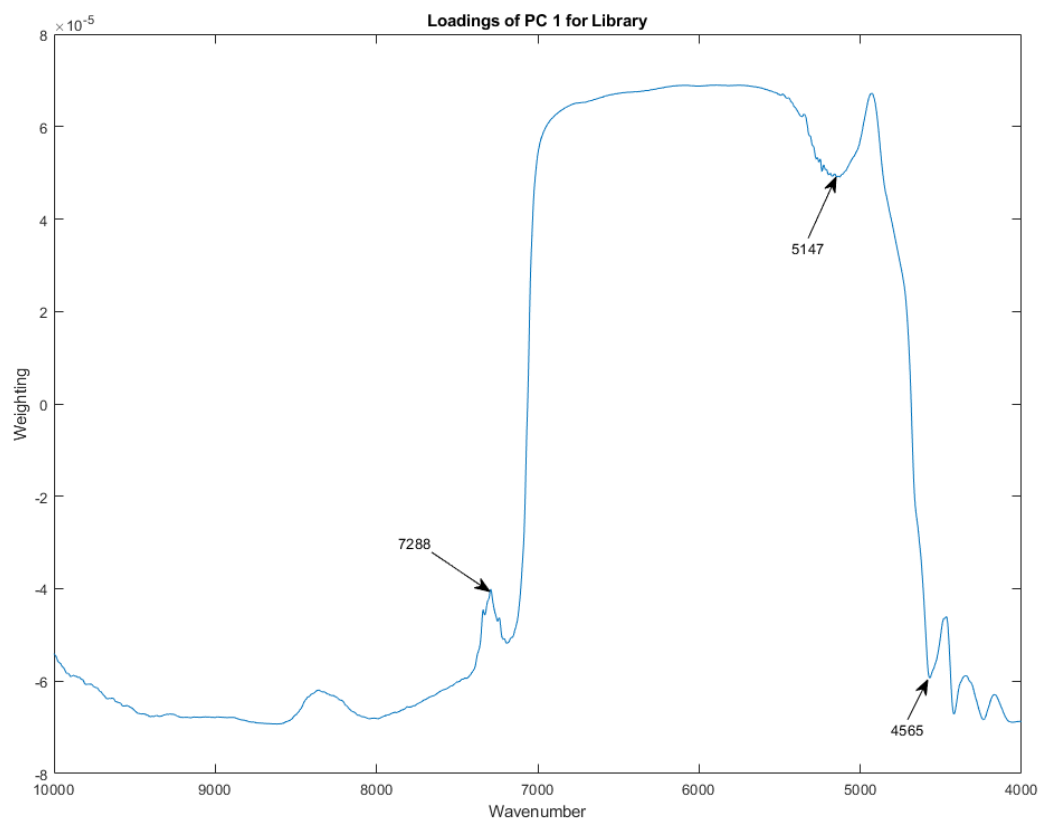


Figure 11. Principal component loadings for PC1 of the abatacept-maltose library.

Principal component loadings for PC1 of the abatacept-maltose library are given in [Figure 11](#). As usual, the first principal component is dominated by baseline variations in the near-infrared spectra of the vials. This means that the first principal component mostly captures the overall position and size of the spectra, rather than any specific chemical features. The signal at 5147 cm^{-1} is probably due to moisture, as this is a common absorption band for water. Notable spectral features appear at 4565, 5147, and 7288 cm^{-1} .

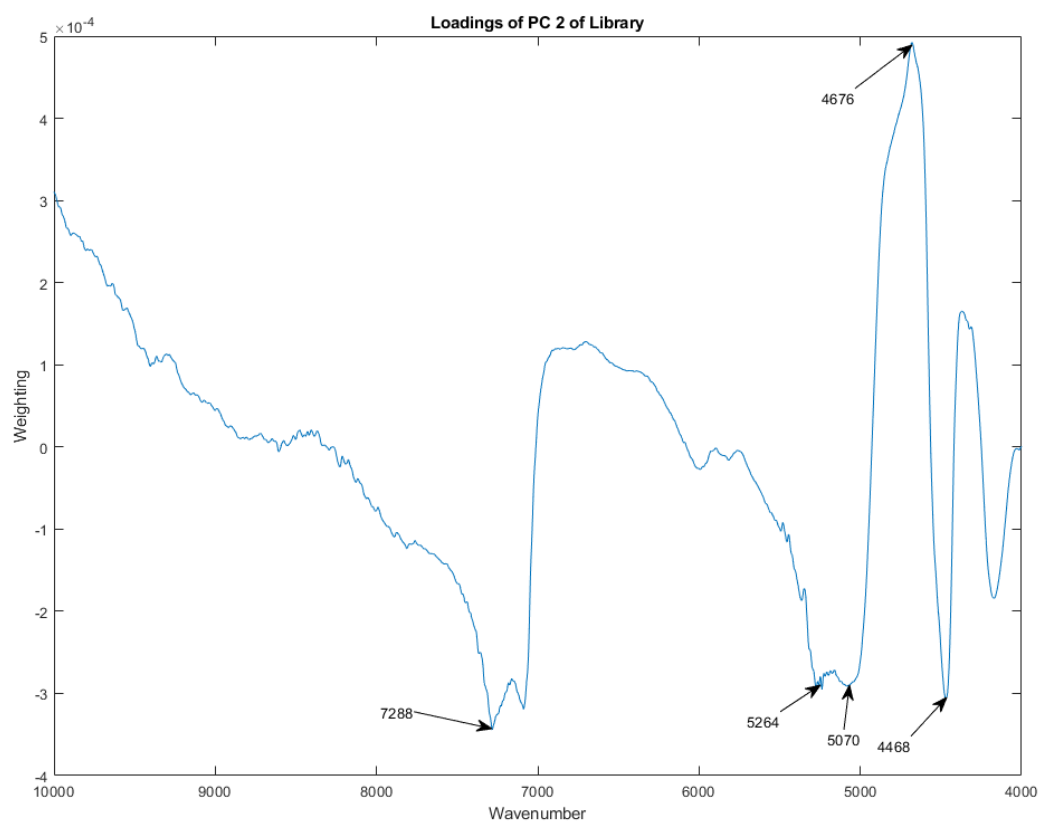


Figure 12. Principal component loadings for PC2 of the abatacept-maltose library.

The principal component loadings for PC2 of the abatacept-maltose library are plotted in [Figure 12](#). The peaks at PC2 show more chemical information than the peaks at PC1, which are more dominated by baseline variations from the vials. Notable spectral features appear at 4468, 4676, 5070, 5264, and 7288 cm^{-1} . The loadings peaks at 4468 and 5070 cm^{-1} represent inversely correlated changes in the library spectra data to the spectral peak at 4676 cm^{-1} . This means that when the peak at 4676 cm^{-1} is high, the peaks at 4468 and 5070 cm^{-1} are low, and vice versa. This information can be used to help identify different compounds in the library.

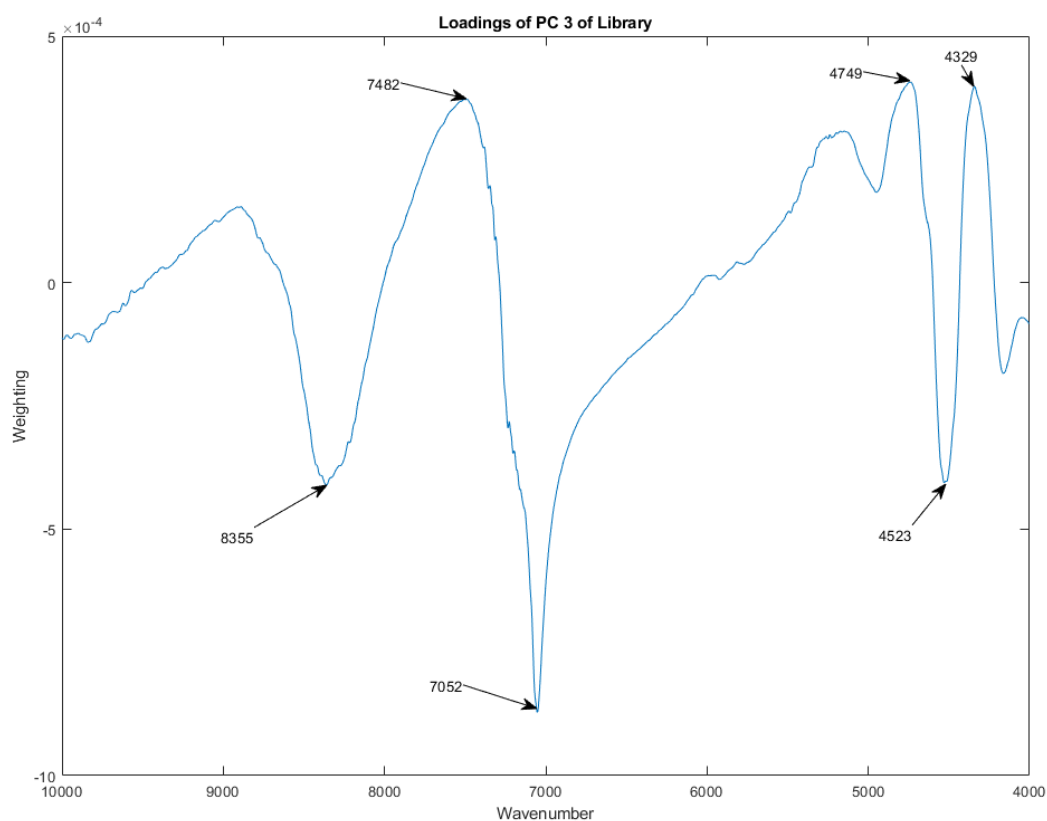


Figure 13. Principal component loadings for PC3 of the abatacept-maltose library.

[Figure 13](#) graphs the PC loadings for PC3 of the abatacept-maltose library. Notable spectral features are observed at 4329, 4523, 4749, 7052, 7482, and 8355 cm^{-1} . PCs 2 and 3 capture the majority of the interesting chemical information present in the spectra of the library.

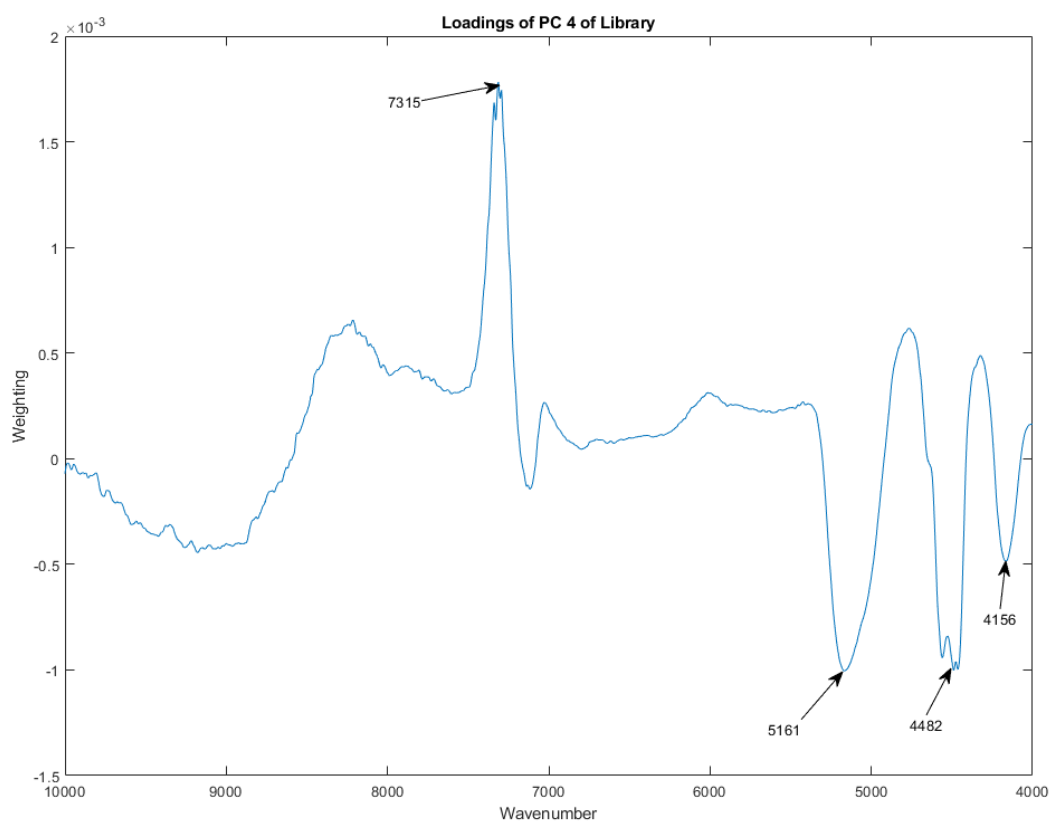


Figure 14. Principal component loadings for PC4 of the abatacept-maltose library.

Principal component loadings for PC4 of the abatacept-maltose library are plotted in [Figure 14](#). By PC4 most of the wavenumbers have near zero weight. Baseline variations are no longer a factor in PC appearance. Interesting spectral features are found at 4156, 4482, 5161, and 7315 cm^{-1} .

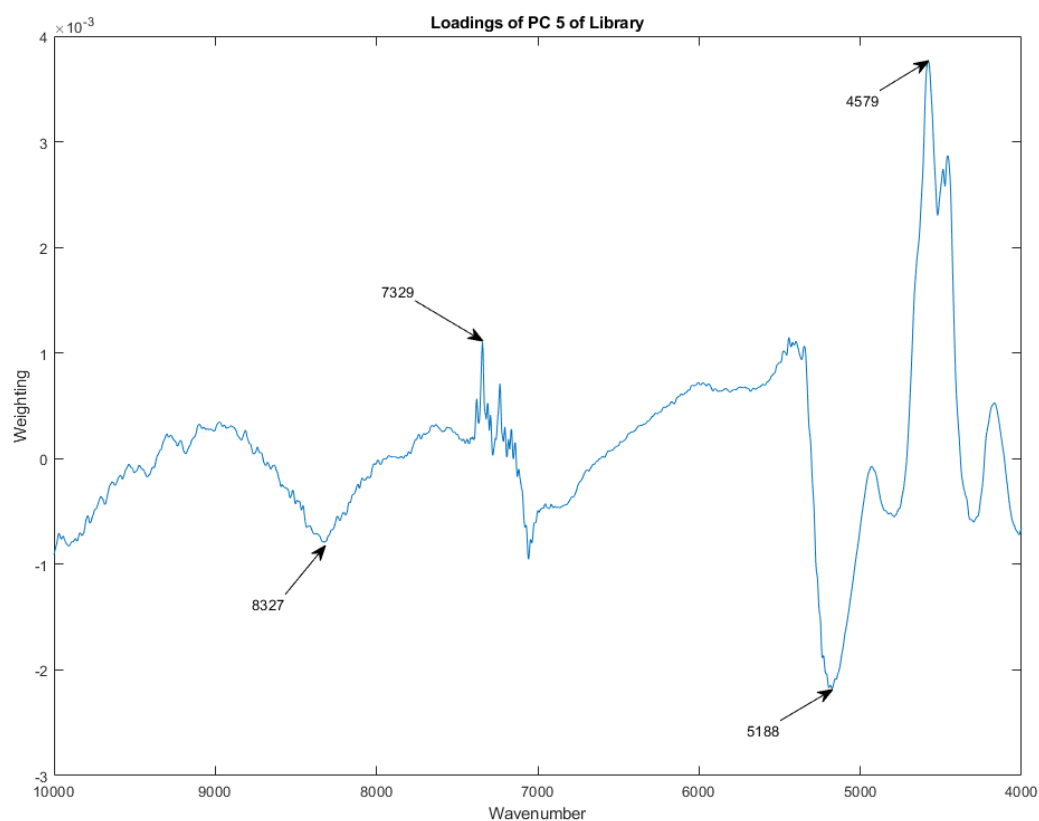


Figure 15. Principal component loadings for PC5 of the abatacept-maltose library.

[Figure 15](#) shows the principal component loadings for PC5 of the abatacept-maltose library. The loadings are a measure of how much each wavenumber contributes to the principal component. The loadings start to become noisy at high wavenumbers and this effect moves even more toward lower wavenumbers at even higher PCs. This suggests that the higher wavenumbers are becoming less important for explaining the variance in the data. The notable spectral features appear at 4579, 5188, 7329, and 8327 cm^{-1} .

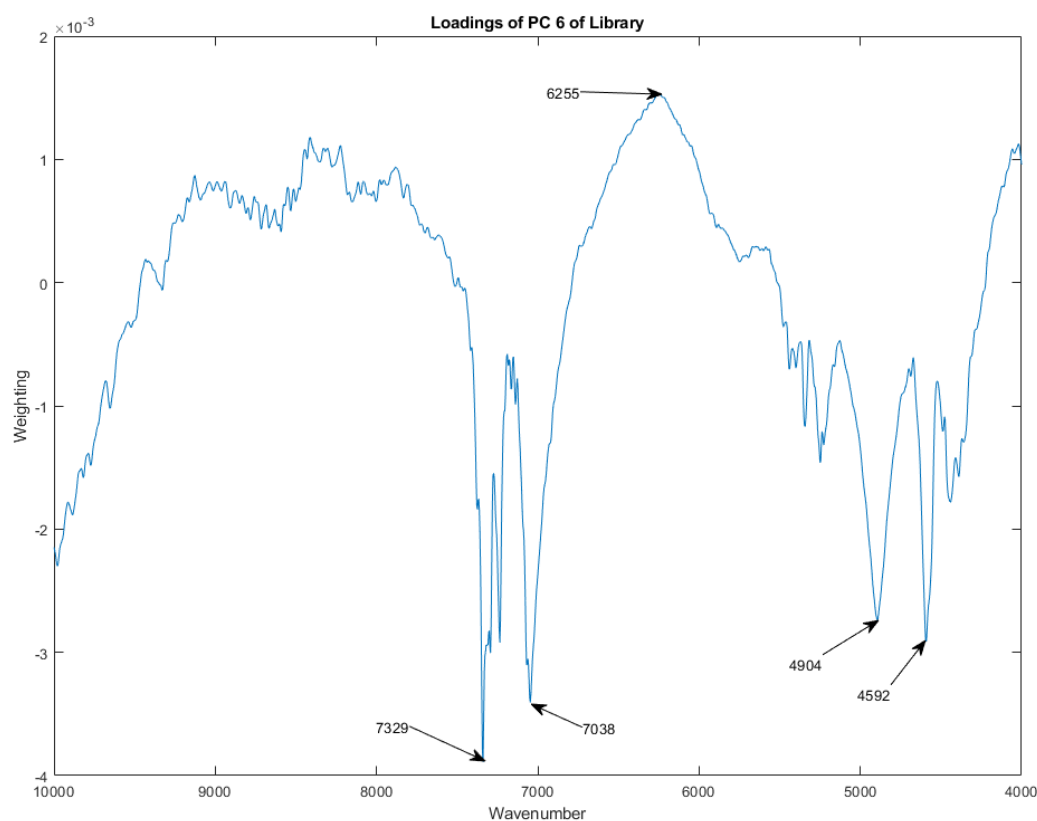


Figure 16. Principal component loadings for PC6 of the abatacept-maltose library.

Principal component loadings for PC6 of the abatacept-maltose library are graphed in Figure 16. By PC 6 there is a considerable amount of noise in the loadings of the library spectra, but PC 6 accounts for only 0.25 percent of the total spectral variation (see [Table 1](#)). Noteworthy spectral features appear at 4592, 4904, 6255, 7038, and 7329 cm^{-1} .

Conclusion

Abatacept is a medication used for the treatment of rheumatoid arthritis and polyarticular juvenile idiopathic arthritis, as well as adult patients with active psoriatic arthritis and acute graft versus host disease. It is administered through intravenous infusion using a sterile, white, preservative-free, freeze-dried powder. Each vial of the drug contains 250 mg of abatacept, along with maltose, monobasic sodium phosphate, and sodium chloride. Abatacept is a fusion protein that combines the extracellular domain of CTLA-4 with the modified Fc portion of human immunoglobulin G1. This fusion protein is produced using recombinant DNA technology.

Abatacept can be used as monotherapy or in combination with other disease-modifying antirheumatic drugs or methotrexate.

There has been variability detected among different lots of abatacept-maltose vials. The University of Kentucky Drug Quality Task Force identified an outlier group of 13 vials from a library of 132 vials across 34 lots. These 13 vials showed significant deviation from the rest of the library cluster. Five of these vials were individually more than 4 standard deviations away from the cluster. This variability may have implications for the consistency and effectiveness of the medication. These spectrometric results do not prove an excess level of impurities or adulteration. However, they suggest that the manufacturing process may have been operating outside of a state of process control. Additional investigation is needed.

Acknowledgements

The project described was supported in part by the National Center for Research Resources and the National Center for Advancing Translational Sciences, National Institutes of Health, through Grant UL1TR001998. The content is solely the responsibility of the authors and does not necessarily represent the official views of the NIH.

References

- BMS, 2021. Orenzia “Highlights Of Prescribing Information,” https://packageinserts.bms.com/pi/pi_orencia.pdf, retrieved Aug. 28, 2023.
- Dempsey, R. J., Davis, D. G., Buice Jr, R. G., & Lodder, R. A. (1996). [Biological and medical applications of near-infrared spectrometry](#). *Applied Spectroscopy*, 50(2), 18A-34A.
- Drug Shortages Canada (2021). <https://www.drugshortagescanada.ca/shortage/146256>. Retrieved Aug. 20, 2023
- FDA, 2013. Orenzia “Highlights Of Prescribing Information” https://www.accessdata.fda.gov/drugsatfda_docs/label/2013/125118s171lbl.pdf, Retrieved Aug. 20, 2023
- Isaacs, J. T., Almeter, P. J., Henderson, B. S., Hunter, A. N., Platt, T. L., & Lodder, R. A. (2023a). [Variability in Content of Hydrocortisone Sodium Succinate](#). Contact in context. DOI:10.6084/m9.figshare.23573532
- Isaacs, J. T., Almeter, P. J., Henderson, B. S., Hunter, A. N., Platt, T. L., & Lodder, R. A. (2023b). [Quality Variations in Thyrotropin Alfa](#). Contact in context. DOI:10.6084/m9.figshare.23524530

Isaacs, J. T., Almeter, P. J., Henderson, B. S., Hunter, A. N., Platt, T. L., & Lodder, R. A., (2023c). [Nonparametric Subcluster Detection in Large Hyperspaces](#), Contact in context. DOI:10.6084/m9.figshare.23877213

Isaksson, T., & Næs, T. (1988). The effect of multiplicative scatter correction (MSC) and linearity improvement in NIR spectroscopy. Applied Spectroscopy, 42(7), 1273-1284. <https://doi.org/10.1366/0003702884429869>

Jolliffe, I. T., & Cadima, J. (2016). [Principal component analysis: a review and recent developments](#). Philosophical Transactions of the Royal Society A: Mathematical, Physical and Engineering Sciences, 374(2065), 20150202.

Lodder, R. A., & Hieftje, G. M. (1988). [Detection of subpopulations in near-infrared reflectance analysis](#). Applied spectroscopy, 42(8), 1500-1512.

Matlab. Smoothing Splines. <https://www.mathworks.com/help/curvefit/smoothing-splines.html>. Retrieved May 28, 2023.

Moustafa, A. S. Z., Spencer, S. K., Bowles, T., Griffin, A., & Wallace, K. (2023). [Different pharmacological agents effects on hypertension attenuation and placental growth factors in an animal model](#). American Journal of Obstetrics & Gynecology, 228(1), S593.

Pollock, D. S. G. (1993). Smoothing with cubic splines. <https://www.physics.muni.cz/~jancely/NM/Texty/Numerika/CubicSmoothingSpline.pdf>. Retrieved May 28, 2023.

TGA (Therapeutic Goods Administration) (2022) Shortage of abatacept (Orencia) medicines. July 4, 2022. <https://www.tga.gov.au/safety/shortages/medicine-shortage-alerts/shortage-abatacept-orencia-medicines>, Retrieved August 15, 2023.

Tsuboi, H., Toko, H., Honda, F., Abe, S., Takahashi, H., Yagishita, M., ... & Sumida, T. (2023). [Abatacept ameliorates both glandular and extraglandular involvements in patients with Sjögren's syndrome associated with rheumatoid arthritis](#): Findings from an open-label, multicentre, 1-year, prospective study: The ROSE (Rheumatoid Arthritis with Orencia Trial Toward Sjögren's Syndrome Endocrinopathy) and ROSE II trials. Modern rheumatology, 33(1), 160-168.

Wu, X. (2023). [Analysis of efficacy and safety of abatacept for rheumatoid arthritis](#): systematic review and meta-analysis. Clinical and Experimental Rheumatology. 07 Mar 2023, DOI: 10.55563/clinexprheumatol/2xjg0d PMID: 36912326